Reports

Geomagnetic Intensity: Changes during the Past 3000 Years in the Western Hemisphere

Abstract. *A series of archeomagnetic measurements have been carried out on archeologic materials from Arizona and Mexico which can be compared with results from Europe and Asia. This comparison shows a westward drift of geomagnetic intensity at a rate of about 0.24 degree per year. Furthermore, an apparent coincidence between changes in the earth's magnetic moment and changes in the production rate of radiocarbon is observed.*

Archeomagnetic investigations carried out in several locations on the Eurasian continent showed that the earth's magnetic intensity has changed during the past 8000 years (*1*). Until now it has not been possible to consider these changes in terms of their worldwide character because of the lack of sufficient data from the Western Hemisphere. Consequently, it was not possible to study a suspected westward drift of the nondipole field in the past. It is our purpose to report now on changes in geomagnetic intensity during the last 3000 years in the Western Hemisphere on the basis of archeological samples, the ages of which were determined by historic, radiocarbon, or stratigraphic-stylistic methods. One significant result of this study was the determination that the nondipole field influenced to a considerable extent the behavior of the geomagnetic intensity in the past.

A total of 80 archeologic and historic samples that we studied were obtained from three localities in Arizona and seven in Mexico (Table 1). The known ages of these materials vary, depending on the origin of the samples and the methods used in determining their ages. For those samples whose temporal placement depends on stylistic criteria, for example, association with certain horizon markers, the possible error in age may be considerable. On the other

Table 1. Ages, magnetic values, and types of samples from Arizona and Mexico; F/F_0 is the ratio of the magnetic field in the past to that of the present field; S, stratigraphic; SS, stratigraphic-stylistic; H, historic; ST, stratigraphic (association of trade sherds); SCP, stratigraphic [association with C^{14} and paleomagnetic orientation data (*5*)]; SCPT, stratigraphic (association with C^{14}, paleomagnetic orientation data, and trade sherds); SPT, stratigraphic (association with paleomagnetic orientation and trade sherds); and W-D, wattle-and-daub material.

Sample No.	Provenience	Geographic coordinates (in deg)	Sample type	Age	Method of determination	F/F_0
			*Mexican samples**			
1.	Morett, Colima	104W,19N	W-D	830 ± 280 B.C.	C^{14} (UCLA 796)†	1.067, 0.987, 1.157
2.	Morett, Colima		W-D	825 ± 225 B.C.	C^{14} (UCLA 799)†	1.140, 1.153
3.	Mexico, D.F. (Cuahtitlan)		Ceramic	100–300 B.C.	S	1.142, 1.250
4.	Morett, Colima		W-D	A.D. 1 ± 170	C^{14} (UCLA 798)†	1.404
5.	Morett, Colima		Ceramic	A.D. 100 ± 200	C^{14} (UCLA 911)†	1.880, 1.870
6.	Morett, Colima		Ceramic	A.D. 1–100	S	1.200
9.	Morett, Colima		Ceramic	A.D. 325 ± 100	C^{14} (UCLA 912)†	1.568
10.	Morett, Colima		Ceramic	A.D. 500–700	SS	0.990, 1.222
11.	Morett, Colima		Ceramic	A.D. 500–700	SS	1.038, 1.148
12.	Tula, Hildago	99.3W,20.6N	Ceramic	A.D. 800–900	SS	1.192, 1.190
13.	Tizapan el Alto, Jalisco	103.1W,19.8N	Ceramic	A.D. 900–1100	SS	1.258, 1.248
14.	Tizapan el Alto, Jalisco		Ceramic	A.D. 900–1100	SS	1.383
15.	Amapa, Nayarit	105.3N,22.1N	Ceramic	A.D. 1000–1100	SS	1.593
16.	Amapa, Nayarit		Ceramic	A.D. 1200–1500	SS	1.468, 1.380
17.	Central Mexico (Aztec)		Ceramic	A.D. 1300–1500	SS	1.255
21.	Morett, Colima		Ceramic	A.D. 150–750	S	0.925
31.	Morett, Colima		Ceramic	300 B.C.–A.D. 100	S	1.098
32.	Playa del Tesoro	103.8W,18.4N	Ceramic	A.D. 150–750	S	1.644
34.	Playa del Tesoro		Ceramic	300 B.C.–A.D. 100	S	1.950
40.	Morett, Colima		Ceramic	300 B.C.–A.D. 100	S	1.085
			Arizona samples			
41.	Tucson		Bricks	A.D. 1920	H	1.000, 1.030
42.	Tucson	111.5W,32.7N	Bricks	A.D. 1780		1.140, 1.153
43.	Snaketown	112.8W,33.9N	Ceramics	300 B.C.–A.D. 1	SCP	1.245, 1.180, 1.063
44.	Snaketown		Ceramics	100 B.C.–A.D. 100	SCP	1.130, 0.833
44a.	Snaketown		Ceramics	100 B.C.–A.D. 100	SCP	1.568
45.	Snaketown		Ceramics	A.D. 100–300	SCP	1.410, 1.468
46.	Snaketown		Ceramics	A.D. 300–500	SCP	1.220
47.	Snaketown		Ceramics	A.D. 500–700	SCPT	1.142, 0.926
48.	Snaketown		Ceramics	A.D. 700–900	SPT	0.744, 1.200, 1.010
49.	Snaketown		Ceramics	A.D. 900–1100	SCPT	1.271, 1.254
50.	Snaketown		Ceramics	A.D. 900–1100	SCPT	1.402, 1.348, 1.506
52.	Snaketown		Ceramics	A.D. 1200–1400	SPT	1.453, 1.222
53.	Pima	109.8W,32.9N	Ceramics	A.D. 1850–1900	ST	1.004

* Paleomagnetic values for 16 archeological samples have not been included in this table because of excessive uncertainties in their known-age values.
† C^{14} values have been calibrated against values for wood dated by the tree-ring method (*8*).

hand, some of the age estimates for ceramic materials from West Mexican sites are more accurately fixed because of association with C^{14} dates, even though the specific assignment of age to the sample in question was made on stylistic or stratigraphic grounds (*2*). Five of the samples utilized for paleomagnetic examination, all from the site of Morett, Colima, were derived from sherd lots dated directly by the radiocarbon content of the organic component of these sherds (*3*).

Eleven of the 13 Arizona samples came from Snaketown, a 300-acre (121-hectare) village of the Hohokam Indians in the Gila River Valley, south-central Arizona (*4*). The relative developmental order of the ten archeological samples measured was established by stratigraphy. Age assignments after A.D. 500 were based on the association of the samples with trade pottery from northern Arizona which has been dated by tree rings. Ages before A.D. 500 were derived by a combination of radiocarbon and paleomagnetic direction (*5*) results, the latter coming from studies of fired clay in hearths and estimates of cultural advancement based on the rate of change after A.D. 500.

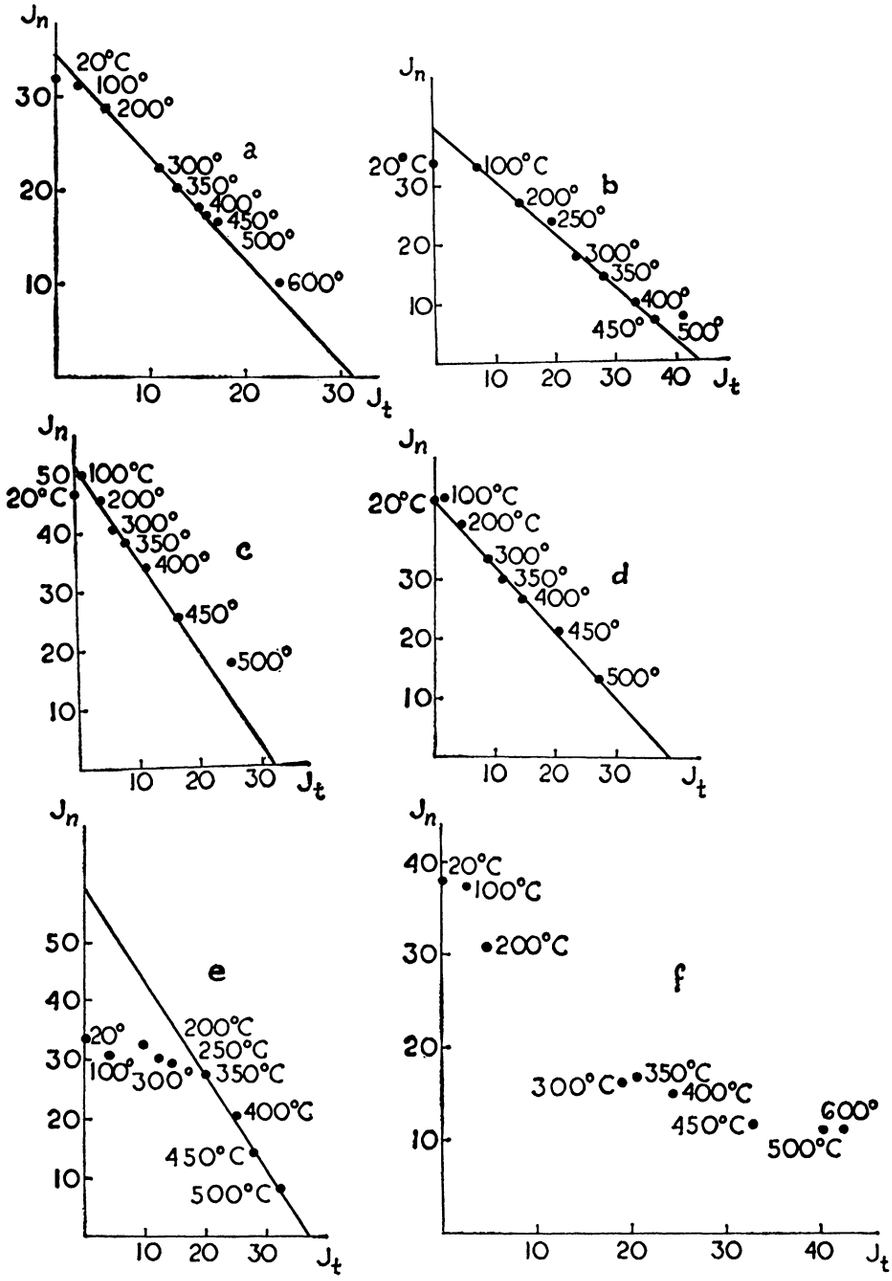

Fig. 1. Temperature dependence of natural remanent magnetization and partial thermoremanent magnetization acquired in the laboratory magnetic field between T and T_0 (room temperature). The following samples are given in J_n–J_t diagrams: (a) No. 41, (b) No. 10, (c) No. 50, (d) No. 1, (e) temperature dependence of natural remanent magnetization including viscous component and partial thermoremanent magnetization, and (f) temperature nonlinear dependence (J_n–J_t diagram) due to disturbing components.

For archeomagnetic analysis the double-heating technique was employed. This method is based on the fact that the thermoremanent magnetization of sherds, wattle-and-daub, and other baked clay is proportional to the intensity of the geomagnetic field in which these objects cooled down from heating. The ratio of the ancient and present-day fields is obtained by comparing the strength of the thermoremanent magnetization in the archeological baked sample with the value acquired after reheating in the present-day geomagnetic field. For reliable results, the whole specimen must have been baked originally up to the same elevated temperature. Experience has shown that no gray or black-colored samples can be used because of their magnetic instability during successive heating up to 600°C.

Measurements of the thermoremanent magnetization were made on an astatic magnetometer in the Geophysical Institute in Prague (*1*). For heat treatment, samples were heated successively in a nonmagnetic oven to temperatures of 100°, 200°, 250°, 300°, 350°, 400°, 450°, and 500°C, first in the direct and then in the reversed position for each temperature. Some were heated to 600°C when the remanent magnetization was very high. The method used for evaluation of the results has been described (*1*). Both magnetization and demagnetization curves for some typical samples are given in Fig. 1, a to d. They show reliable determinations of the ratio F/F_0* (ratio of the magnetic field in the past to that in the laboratory field) which is the coefficient (k) defined by the ratio of sections on axes J_n, J_t for different values and ages within the time period investigated. The example in Fig. 1a, for a specimen dating from A.D. 1920, verifies the method applied because it acquired its thermoremanent magnetization in a known magnetic field. The ratio of the magnetic field in the past

to the present-day field in the locality (F/F_0) agrees with the value obtained by dividing the measured field in A.D. 1920 by the present-day magnetic field. One further example (Fig. 1e) shows the influence of viscous magnetization or some other less stable magnetization which originated in the sherd after it was manufactured. In such cases it is still possible to determine the ratio F/F_0*. However, when the linear dependence is defined by less than four points along the line (Fig. 1f), it is not possible to find an unambiguous interpretation, and results cannot be utilized. This usually applies to samples of gray or black color, or when the sample was heated during manufacture to temperatures of >1000°C causing conversion of hematite into magnetite.

Results of archeomagnetic measurements of samples from Arizona and Mexico are given in Table 1. The majority of samples (72) could be utilized. Upon examination, only eight showed inconsistent, nonlinear dependences due mainly to mineralogical changes during successive heating. The temporal dependence of ratios F/F_0 is given in Fig. 2a for Arizona and in Fig. 2b for Mexico. The ratio between laboratory magnetic field and present geomagnetic field, that was used for recalculation of F_0* to F_0, amounted to 0.926 for Arizona and 1.067 for Mexico [laboratory field was 47,500 γ; present field in Tucson was 51,300 γ and in Teloyucan 44,500 γ (1 gamma = 0.00001 oersted)]. The Arizona (Snaketown) samples provided a sequence gradually increasing in age, thus making it possible to observe the basic course of magnetic field changes of the earth during the past 2000 years. Although the known ages of the Mexican samples were not always as precise, a similar dependence in the nondipole field was observed.

When the archeomagnetic results from Arizona and Mexico are compared with the data from Europe, the course of geomagnetic intensity changes can be deduced. It appears from Fig. 3 that there were changes that took place in shorter periods of time so that their maximum and minimum values are shifted in time with respect to each other. Because precise dating of some samples was not always possible, a measure of uncertainty exists in the exact course of some portions of the curves. When European and American results are compared (*6*), a definite westward shift between maximum

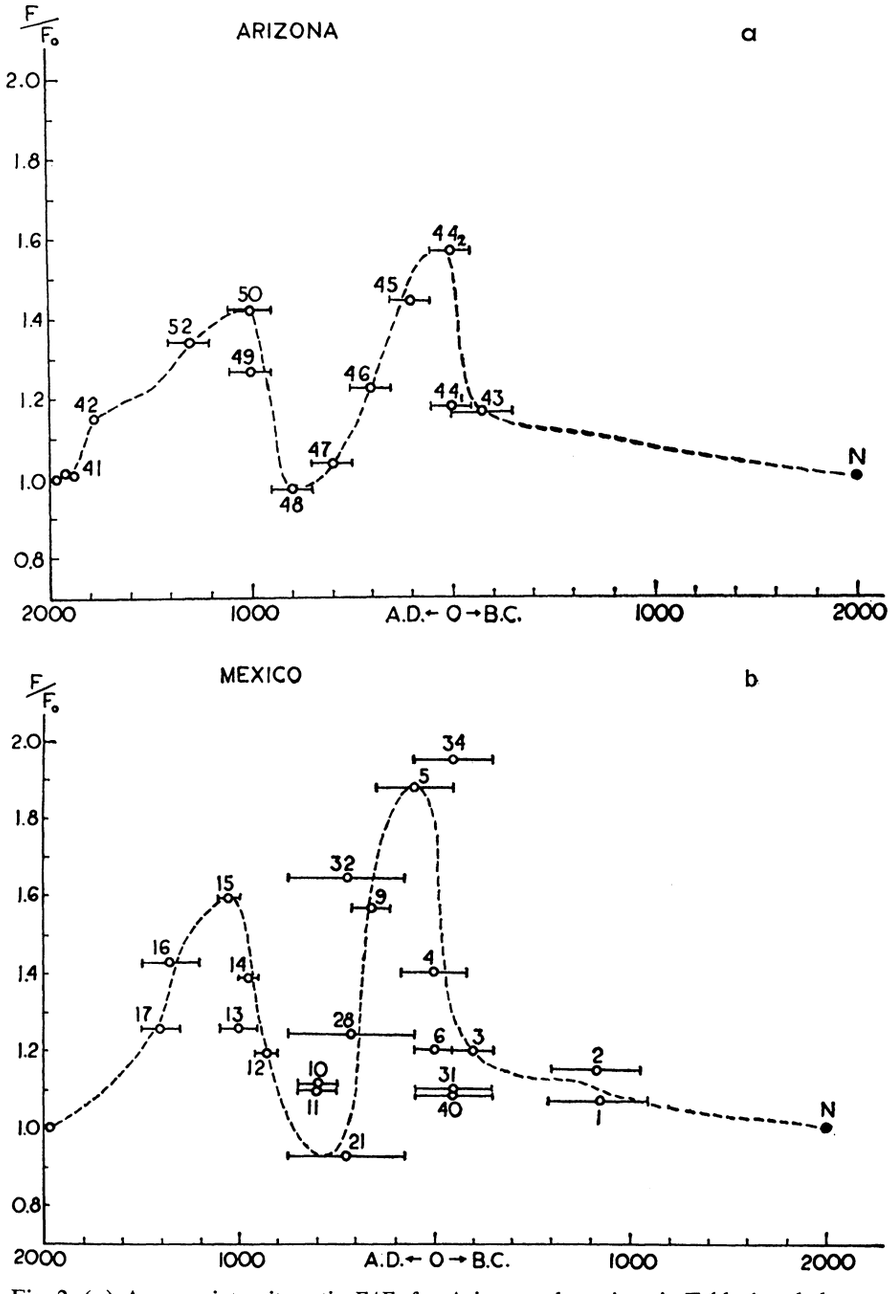

Fig. 2. (a) Average intensity ratio F/F_0 for Arizona values given in Table 1 and changes of the geomagnetic field during the past 4000 years; N, value according to Kitazawa and Kobayashi (*11*). (b) Average intensity ratio F/F_0 for Mexico (Table 1).

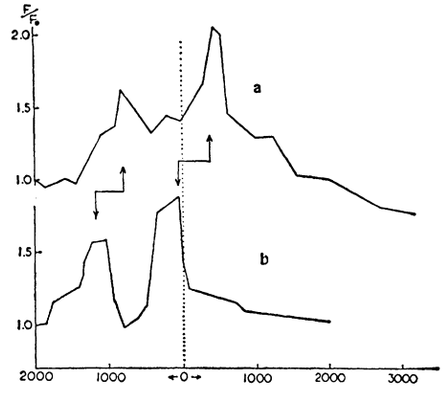

Fig. 3. Archeomagnetic curves for Czechoslovakia (a) and Central America (b) showing westward drift of maximum and minimum values of the nondipole field (shift is given by arrows).

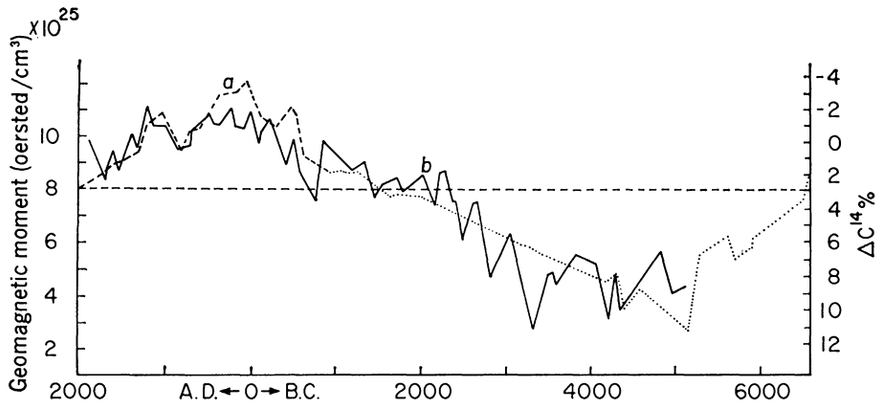

Fig. 4. Comparison of C^{14} deviations for the half-life 5730 years according to Suess (*9*) (curve b) with the geomagnetic moment changes (curve a) (*6*). Dashed portion of the curve represents average changes determined from values in Europe, Central America, and Japan; dotted curve is for changes from Europe only.

values can be detected, which amounts to a shift rate of approximately 120° of longitude in 500 years or 0.24° per year. This value corresponds very well with the values determined on the basis of direct geomagnetic field measurements by geophysical observatories and geomagnetic mapping during the past century (*7*).

Archeomagnetic measurements of South American pottery (*8*) show that a similar increase in intensity took place during approximately the same time period. Moreover, when archeomagnetic results from America, Europe, and Japan are taken into account, it is possible to calculate values for the earth's magnetic moment of the archeological past (*6*). These values show a very good inverse coincidence (Fig. 4) with secular fluctuations in the production rate of radiocarbon reported earlier by Suess (*9*). Since archeomagnetic measurements have made it possible to detect the apparently direct dependence between changes of the earth's magnetic moment and changes in the production rate of radiocarbon, any possible influence of the earth's magnetic field during the last 40,000 years can be estimated by conducting magnetic paleointensity measurements on sediments that are datable by the radiocarbon method. The experiments reported here should go a long way toward clarifying the relative effectiveness of the magnetic behavior of the earth and sun and their influence on the production rate of radiocarbon as discussed recently by Libby (*10*). Finally, there remains the interesting aspect that a redefinition of the mean radiocarbon concentration in the biosphere, in the light of variations in the production of C^{14} with time, might present a different view of the extent of maximum deviation, which might be cut in half.

V. Bucha*

Geophysical Institute of Czechoslovak Academy of Science, Prague

R. E. Taylor†, Rainer Berger

Department of Anthropology and *Institute of Geophysics, University of California, Los Angeles*

E. W. Haury

Department of Anthropology, University of Arizona, Tucson

References and Notes

1. V. Bucha, *Archaeometry* **10**, 12 (1967).
2. R. Berger and W. F. Libby, *Radiocarbon* **9**, 477 (1967); S. V. Long and R. E. Taylor, *Science* **154**, 1456 (1966).
3. R. E. Taylor and R. Berger, *Amer. Antiquity* **33**, 363 (1968).
4. H. S. Gladwin, E. W. Haury, E. B. Sayes, N. Gladwin, *Medallion Papers 15*, whole issue (1937).
5. R. D. Bois, in preparation.
6. V. Bucha, in *Proceedings of the 12th Nobel Symposium, Uppsala, August 1969*, in press.
7. E. Bullard, C. Freedman, H. Gellman, J. Nixon, *Phil. Trans. Roy. Soc. London Ser. A* **243**, 67 (1951).
8. T. Nagata, K. Kobayashi, E. J. Schwarz, *J. Geomag. Geoelec.* **17**, 399 (1965).
9. H. E. Suess, *J. Geophys. Res.* **70**, 5937 (1965); *Bild Wiss.* **6**, 121 (1969).
10. W. F. Libby, in *Proceedings of a Symposium on Radioactive Dating and Methods of Low-Level Counting, Monaco, 2–10 March 1967* (International Atomic Energy Agency, Vienna, 1967), pp. 3–25.
11. K. Kitazawa and K. Kobayashi, *J. Geomag. Geoelec.* **20**, 7 (1968).
12. We thank A. Kalenska and M. Prosova for competent experimental assistance, and W. F. Libby, C. W. Meighan, and H. E. Suess for encouragement. Supported by NSF grants GA-4349 and GA-1641. Publication No. 750 of the Institute of Geophysics and Planetary Physics, University of California, Los Angeles.

* Present address: Institute of Geophysics, University of California, Los Angeles and San Diego.
† Present address: Department of Anthropology, University of California, Riverside.

13 November 1969

Polywater: An Attempt at Synthesis in a Gas Discharge

Abstract. *An attempt to produce polywater in a corona discharge in moist air was unsuccessful. However, the major product produced, nitric acid, has a midrange infrared spectrum which is strikingly similar to that reported for polywater. The Raman spectrum offers a better means of distinguishing between nitric acid and polywater than the infrared spectrum does.*

Recently, Lippincott *et al.* (*1*) have presented evidence that the "anomalous water" studied extensively by Deryagin and Churayev (*2*) is a well-defined polymeric form of water. Polywater is most commonly prepared by condensing ordinary water in freshly drawn glass capillaries. The small quantities produced by this method have hampered precise characterization of the properties of the material and have led us to consider alternate methods of preparation.

Experiments by Shahin (*3*) and others have established that the principal charge carriers in a positive corona discharge in moist air are species of the form $(H_2O)_nH^+$, where n has been observed to vary from 1 to 9 under typical conditions. The detailed structure of the ions has not been determined; however, both simple hydration and more complicated bonding schemes have been suggested (*4*). The similarity in the form of these species to the polymeric form proposed by Lippincott *et al.* suggested that polywater might be a product of a positive corona discharge in moist air. Fowkes (see *5*) has observed that strong electric fields are known to exist at freshly drawn glass surfaces. It has been suggested that the role of the electric field is to attract water molecules to the glass surface where the molecular arrangement provides a "pattern" for the formation of polywater by a sort of epitaxial growth. We speculated, however, that the surface fields might be adequate to produce air breakdown in the capillary and that the polywater could be formed in the resulting discharge.

We initiated experiments designed to collect and identify the products of a positive corona discharge in moist air. The apparatus used consisted of an O-ring-sealed Pyrex vessel with an internal volume of about 1 liter enclosing a corona device of coaxial cylinder geometry. The relative humidity in the vessel was maintained at 100 percent